Effects of Viscous Dissipation and Joule Heating on Natural Convection Flow of a Viscous Fluid from Heated Vertical Wavy Surface

Nasser S. Elgazery[a] and Nader Y. Abd Elazem[b]

Department of Mathematics, Faculty of Education, Ain Shams University, Roxy, Heliopolis, Cairo, Egypt

[a] Present Address: Department of Mathematics, Deanship of Educational Services, Al-Qassim University, P.O. Box 6595, Al-Qassim, Buraidah, 51452 Saudi Arabia

[b] Present Address: Department of Mathematics, Faculty of Science, Tabuk University, P.O. Box 741, Tabuk 71491, Saudi Arabia

Reprint requests to N.Y. A.E.; E-mail: naderelnafrawy@yahoo.com

Z. Naturforsch. **66a,** 427 – 440 (2011); received July 3, 2010 / revised November 30, 2010

A mathematical model will be analyzed in order to study the effects of viscous dissipation and Ohmic heating (Joule heating) on magnetohydrodynamic (MHD) natural convection flow of a temperature dependent viscosity from heated vertical wavy surface. The present physical problem is studied numerically by using the appropriate variables, which reduce the complex wavy surface into a flat one. An implicit marching Chebyshev collocation scheme is employed for the analysis. Numerical solutions are obtained for velocity, temperature, local skin friction, and Nusselt number for a selection of parameter sets consisting of Eckert number, Prandtl number, MHD variation, and amplitude-wavelength ratio parameter. Numerical results show that these parameters have significant influences on the velocity and the temperature profiles as well as for the local skin friction and Nusselt number.

Key words: Wavy Surface; Magnetohydrodynamic; Viscous Dissipation; Chebyshev Collocation Method.

PACS numbers: 47.11.-j; 47.11.kb

1. Introduction

The natural convection about a heated vertical wavy surface has received a great deal of attention due to its relation to practical applications of complex geometries. The electric and magnetic fields must obey a set of physical laws, which are expressed by Maxwell's equations. The solution to such problems requires the simultaneous solution for the set of fluid mechanics and electromagnetism equations. Through the studied cases there is a special case of this type of coupling known as magnetohydrodynamic (MHD). Many works on heat transfer have focused mainly on regular geometries, few studies have been carried out to examine the effect of geometric complexity, such as irregular surfaces, on the convection heat transfer. That is because complicated boundary conditions or external flow fields are difficult to deal with. The natural convection along a wavy surface, such as sinusoidal surfaces, have been studied by Yao [1], Moulic and Yao [2], Rees and Pop [3], Pop and Na [4]. They solved the transformation boundary layer equations of the natural convection in Newtonian fluids by a numerical finite difference method. Results show that the local heat transfer rates vary periodically along the wavy surface, with a frequency equal to twice the frequency of the wavy surface. Recently, Jang et al. [5 – 7] investigated natural or mixed convection heat and mass transfer along a wavy surface. Another interesting application of hydromagnetic to metallurgy lies in the purification of molten metals from non-metallic inclusions by the application of a magnetic field. Developments of new technologies in these areas require both improvements in our ability to create adequate mathematical models and in our understanding of the fundamental physical processes involved in the fluid flow. The sinusoidal wavy surface can be viewed as an approximation to much practical geometries in heat transfer. A good example is a cooling fin. Since cooling fins have a larger area than a flat surface, they are better heat transfer devices. Free convection in a non-Darcian wavy porous enclosure studied by Rathish Kumar and Shalini [8]. Recently, Rathish Kumar and Shalini [9] investigated non-Darcy free convection induced by a vertical wavy surface in a thermally stratified porous medium. Natural convection along a vertical complex wavy surface was studied by Yao [10]. On the other hand, Hossain and Pop [11] investigated the magnetohydrodynamic boundary layer flow and heat transfer along a continuous moving wavy surface. The problem of free-convection flow from a wavy vertical surface in presence of a transverse magnetic field was studied by Hossain et al. [12]. Natural convection flow along a vertical wavy surface with uniform surface temperature in presence of heat generation/absorption was studied by Molla et al. [13]. Hossain and Rees [14] have investigated the combined effect of thermal and mass diffusion on the natural convection flow of a viscous incompressible fluid from a vertical wavy surface. In all the above studies the viscosity of the fluid has been assumed to be constant. However, it is known that this physical property may change significantly with temperature. Kafoussias and Williams [15] and Kafoussias et al. [16] investigated the effect of temperature dependent viscosity on the mixed convection flow from a vertical flat plate in the region near the leading edge using the local non-similarity method. Natural convection flow of a viscous fluid with the viscosity inversely proportional to a linear function of temperature from a vertical wavy cone was investigated by Hossain et al. [17]. Hossain et al. [18] have studied the problem of natural convection of a fluid with variable viscosity from a heated vertical wavy surface. Although these intensive works were done by the above mentioned authors, the effects of viscous dissipation and Ohmic heating on MHD natural convection flow of the Newtonian fluid case were not studied or developed. Consequently, the main purpose of this research is an extension of the work done by Hossain et al. [18]. Hence the purpose of this work is to study the more general problem which includes the effects of viscous dissipation and Ohmic heating on MHD natural convection flow of a Newtonian fluid with a temperature dependent viscosity from a vertical wavy surface in the presence of a magnetic field. The results of the present study are an important process of manufacturing. The prediction of heat transfer from an irregular surface is of fundamental importance and is encountered in several heat transfer devices, such as flat-plate solar collectors and flat-plate condensers in refrigerators. Irregularities frequently occur in the process of manufacturing. Moreover, surfaces are sometimes intentionally roughened to enhance heat transfer because the presence of rough surfaces disturbs the flow and alters the heat transfer rates. There is now a discussion of research performed on some irregular surfaces following. The fluid viscosity is assumed to vary as inversely proportional to a linear function of temperature. The spectral method can yield greater accuracy for a smooth solution with far fewer nodes and therefore less computational time than the finite-difference and finite-element schemes (see Elgazery [19]). The dimensionless nonlinear partial differential equations are solved numerically by using the implicit Chebyshev collocation method. It is hoped that the results obtained will not only provided useful information for applications but also serve as a complement to the previous studies.

2. Mathematical Formulation

Consider the steady, laminar boundary layer in a two-dimensional natural-convection of a Newtonian fluid of a temperature dependent viscosity from a vertical wavy surface. A uniform magnetic field of strength B_0 is imposed along the Y-axis (Fig. 1). The thermo-physical fluid properties are assumed to be isotropic and constant except the buoyancy term in the X momentum equation, the fluid viscosity μ, which was introduced by [20] and which was also used by Kafoussias et al. [16] in the form

$$\mu = \frac{\mu_\infty}{1+\gamma(T-T_\infty)},$$

where γ is a constant and μ_∞, T, and T_∞ are the fluid free-stream dynamic viscosity, the temperature of the fluid in the boundary layer, and the temperature of the fluid far away from the wavy surface, respectively. Also, the temperature at the wavy surface is kept at the constant value T_w of the X-coordinate. The wavy surface of the plate is described in the function

$$Y = \bar{\sigma}(X) = a \cdot \sin(X/L), \tag{1}$$

where a is the amplitude of the wavy surface and L is the wavelength of the wavy surface.

Under the Boussinesq and boundary layer approximations which are used to characterize the buoyancy effect, the governing continuity, momentum, and energy conservation equations are

$$\frac{\partial U}{\partial X} + \frac{\partial V}{\partial Y} = 0, \tag{2}$$

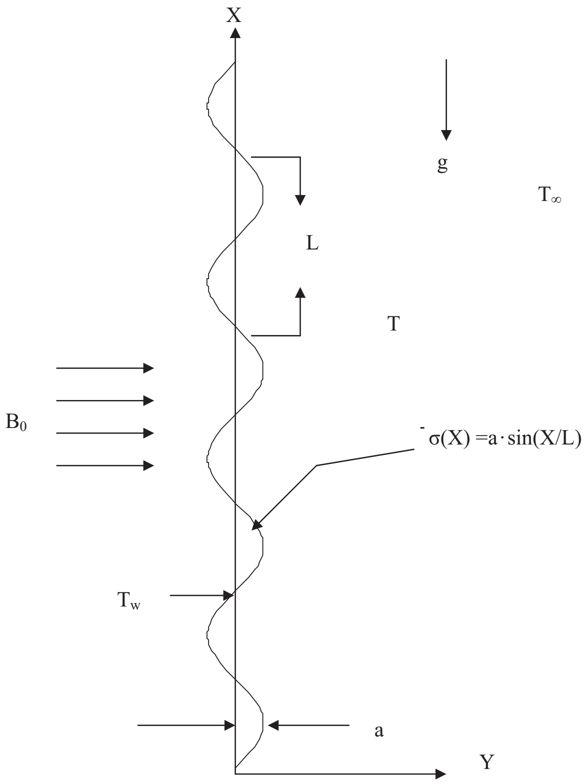

Fig. 1. Schematic diagram of the physical system.

$$U\frac{\partial U}{\partial X}+V\frac{\partial U}{\partial Y}=-\frac{1}{\rho}\frac{\partial P}{\partial X}+g\beta_{\mathrm{T}}(T-T_\infty)-\frac{\sigma^* B_0^2}{\rho}U+\frac{1}{\rho}\left(\frac{\partial}{\partial X}\left(\mu\frac{\partial U}{\partial X}\right)+\frac{\partial}{\partial Y}\left(\mu\frac{\partial U}{\partial Y}\right)\right), \tag{3}$$

$$U\frac{\partial V}{\partial X}+V\frac{\partial V}{\partial Y}=-\frac{1}{\rho}\frac{\partial P}{\partial Y}+\frac{1}{\rho}\left(\frac{\partial}{\partial X}\left(\mu\frac{\partial V}{\partial X}\right)+\frac{\partial}{\partial Y}\left(\mu\frac{\partial V}{\partial Y}\right)\right), \tag{4}$$

$$U\frac{\partial T}{\partial X}+V\frac{\partial T}{\partial Y}=\frac{k_{\mathrm{f}}}{\rho c_{\mathrm{p}}}\left(\frac{\partial^2 T}{\partial Y^2}\right)+\frac{\mu}{\rho c_{\mathrm{p}}}\left(\frac{\partial U}{\partial Y}\right)^2+\frac{\sigma^* B_0^2}{\rho c_{\mathrm{p}}}U^2. \tag{5}$$

The boundary conditions are given by [18]:

$$\begin{cases} U=V=0,\ T=T_{\mathrm{w}} & \text{at } Y=\bar{\sigma}(X), \\ U\to 0,\ T\to T_\infty,\ P\to P_\infty & \text{as } Y\to\infty. \end{cases} \tag{6}$$

Based on the previous equations, (U,V) are the velocity components along the (X,Y) axis, respectively. ρ, β_{T}, P, and P_∞ are the density of the fluid, the volumetric coefficient of the thermal expansion, the pressure of the fluid, and the constant pressure of the ambient fluid, respectively. σ^* is the electrical conductivity. B_0, k_{f}, c_{p}, and g are the applied magnetic field, the fluid thermal conductivity, the fluid specific heat at constant pressure, and the acceleration due to gravity, respectively.

We now introduce the following dimensionless variables:

$$\begin{aligned} &x=\frac{X}{L},\ y=\frac{Y-\bar{\sigma}}{L}\mathrm{Gr}^{\frac{1}{4}},\ u=\frac{\rho L}{\mu_\infty \mathrm{Gr}^{\frac{1}{2}}}U,\\ &v=\frac{\rho L}{\mu_\infty \mathrm{Gr}^{\frac{1}{4}}}(V-\sigma_x U),\ \theta=\frac{T-T_\infty}{T_{\mathrm{w}}-T_\infty},\\ &M=\frac{\sigma^* B_0^2 L^2}{\mu_\infty \mathrm{Gr}^{\frac{1}{2}}},\ p=\frac{L^2}{\rho \nu_\infty^2 \mathrm{Gr}}(P-P_\infty),\\ &\mathrm{Gr}=\frac{g\beta_{\mathrm{T}}(T_{\mathrm{w}}-T_\infty)\rho^2 L^3}{\mu_\infty^2},\ \mathrm{Ec}=\frac{g\beta_{\mathrm{T}} L}{c_{\mathrm{p}}},\\ &\mathrm{Pr}=\frac{\mu_\infty c_{\mathrm{p}}}{k_{\mathrm{f}}},\ \sigma=\frac{\bar{\sigma}}{L}, \end{aligned} \tag{7}$$

where ν_∞ is the fluid free-stream kinematic viscosity, M is the magnetic parameter, Gr is the temperature Grashof number, Pr is the Prandtl number, Ec is the Eckert number, $\bar{\sigma}$ is the coordinate of the wavy surface in (1), and σ is the dimensionless coordinate of the wavy surface.

Introducing expressions (7) into (2)–(5) and ignoring the small-order terms in Gr, the transformed governing equations in the dimensionless form can be obtained as written below:

$$\frac{\partial u}{\partial x}+\frac{\partial v}{\partial y}=0, \tag{8}$$

$$u\frac{\partial u}{\partial x}+v\frac{\partial u}{\partial y}=-\frac{\partial p}{\partial x}+\sigma_x\frac{\partial p}{\partial y}\mathrm{Gr}^{\frac{1}{4}}+\left(\frac{1+\sigma_x^2}{1+\varepsilon\theta}\right)\frac{\partial^2 u}{\partial y^2}-\frac{\varepsilon(1+\sigma_x^2)}{(1+\varepsilon\theta)^2}\left(\frac{\partial u}{\partial y}\right)\left(\frac{\partial\theta}{\partial y}\right)+\theta-Mu, \tag{9}$$

$$\sigma_x\left(u\frac{\partial u}{\partial x}+v\frac{\partial u}{\partial y}\right)+u^2\sigma_{xx}=-\mathrm{Gr}^{\frac{1}{4}}\frac{\partial p}{\partial y}+\sigma_x\left(\frac{1+\sigma_x^2}{1+\varepsilon\theta}\right)\frac{\partial^2 u}{\partial y^2}-\frac{\varepsilon\sigma_x(1+\sigma_x^2)}{(1+\varepsilon\theta)^2}\left(\frac{\partial u}{\partial y}\right)\left(\frac{\partial\theta}{\partial y}\right), \tag{10}$$

$$u\frac{\partial\theta}{\partial x}+v\frac{\partial\theta}{\partial y}=\left(\frac{1+\sigma_x^2}{\mathrm{Pr}}\right)\frac{\partial^2\theta}{\partial y^2}+\left(\frac{\mathrm{Ec}}{1+\varepsilon\theta}\right)\left(\frac{\partial u}{\partial y}\right)^2+M\,\mathrm{Ec}\,u^2. \tag{11}$$

It is noticeable that σ_x, σ_{xx} indicate the first and second differentiations of $\sigma(x) = \alpha \sin(x)$ with respect to x where $\alpha = \frac{a}{L}$ is the amplitude-wavelength ratio, therefore, $\sigma_x = \frac{\mathrm{d}\bar{\sigma}}{\mathrm{d}X} = \frac{\mathrm{d}\sigma}{\mathrm{d}x}$ and $\sigma_{xx} = \frac{\mathrm{d}\sigma_x}{\mathrm{d}x}$. For the current problem, the pressure gradient $\frac{\partial p}{\partial x}$ is zero. Therefore (9) can be reduced to the following equation after eliminating $\frac{\partial p}{\partial y}$ in (9) and (10):

$$u\frac{\partial u}{\partial x}+v\frac{\partial u}{\partial y}=\left(\frac{1+\sigma_x^2}{1+\varepsilon\theta}\right)\frac{\partial^2 u}{\partial y^2}-\frac{\varepsilon\left(1+\sigma_x^2\right)}{(1+\varepsilon\theta)^2}\left(\frac{\partial u}{\partial y}\right)\left(\frac{\partial \theta}{\partial y}\right)+\left(\frac{1}{1+\sigma_x^2}\right)\theta-\left(\frac{\sigma_x\sigma_{xx}}{1+\sigma_x^2}\right)u^2-\left(\frac{M}{1+\sigma_x^2}\right)u. \tag{12}$$

The quantity $\varepsilon = \gamma(T_\mathrm{w} - T_\infty)$ is defined by the viscosity-temperature variation, expressed by the equation $\mu = \frac{\mu_\infty}{1+\gamma(T-T_\infty)}$. It can be seen clearly that the dimensionless viscosity $\frac{\mu}{\mu_\infty}$ lies in the range between $(\frac{1}{1+\varepsilon})$ and 1; its value is decreasing with increasing temperature when $\varepsilon > 0$. The difference $(T_\mathrm{w} - T_\infty)$ is greater than zero $(T_\mathrm{w} > T_\infty)$ (free convection) and $\varepsilon > 0$. This means that γ, the thermal property of the fluid, is positive $(\varepsilon = \gamma(T_\mathrm{w} - T_\infty))$ and hence the fluid must be liquid (e.g. water, $\mathrm{Pr} = 7$) and not a gas (e.g. air, $\mathrm{Pr} = 0.7$) (see Kafoussias and Williams [15]).

Actually, the present work is a continuation and an extension of a work written by Hossain et al. [18], where the fluid viscosity is assumed to vary as an inverse linear function of temperature. Then the expression $\mu = \frac{\mu_\infty}{1+\gamma(T-T_\infty)}$ is used in the present paper whereas in [18] the authors used the wrong expression $\mu = \mu_\infty[1+\gamma(T-T_\infty)]$. So (9) and (10) are correct in the present paper, i.e., in (9), the coefficient of the term $(\frac{\partial u}{\partial y})(\frac{\partial \theta}{\partial y})$ in [18] is $-\frac{\varepsilon}{1+\varepsilon}$ whereas this term is not presented in the corresponding equation (9) in the present work. On the other hand, in (10), in the present work, there is the term (the last term) $-\frac{\varepsilon\,\sigma_x(1+\sigma_x^2)}{(1+\varepsilon\theta)^2}(\frac{\partial u}{\partial y})(\frac{\partial \theta}{\partial y})$, whereas this term is not presented in the corresponding equation (10) of [18].

The boundary conditions are now given by

$$\begin{cases} u=v=0,\;\; \theta=1 & \text{at}\;\; y=0,\\ u\to 0,\;\; \theta\to 0,\;\; p\to 0 & \text{as}\;\; y\to\infty. \end{cases} \tag{13}$$

The following non-similar variables have been introduced:

$$\psi = x^{\frac{3}{4}} f(x,\eta),\;\; \eta=\frac{y}{x^{\frac{1}{4}}},\;\; \theta=\theta(x,\eta), \tag{14}$$

where ψ is the stream function, which satisfies the equation of continuity (8) and which is defined according to $u = \partial\psi/\partial y$ and $v = -\partial\psi/\partial x$.

The boundary layer equations can be obtained as

$$\left(\frac{1+\sigma_x^2}{1+\varepsilon\theta}\right)f'''+\frac{3}{4}f\;f''-\left(\frac{1}{2}+\frac{x\sigma_x\sigma_{xx}}{1+\sigma_x^2}\right)f'^2-\frac{\varepsilon\left(1+\sigma_x^2\right)}{(1+\varepsilon\theta)^2}\theta' f''+\left(\frac{1}{1+\sigma_x^2}\right)\theta-\left(\frac{Mx^{\frac{1}{2}}}{1+\sigma_x^2}\right)f'=x\left(f'\,\frac{\partial f'}{\partial x}-f''\,\frac{\partial f}{\partial x}\right), \tag{15}$$

$$\frac{\left(1+\sigma_x^2\right)}{\mathrm{Pr}}\theta''+\frac{3}{4}f\;\theta'=x\left(f'\frac{\partial\theta}{\partial x}-\theta'\frac{\partial f}{\partial x}-\frac{\mathrm{Ec}}{(1+\varepsilon\theta)}f''^2-M\,\mathrm{Ec}\,x^{\frac{1}{2}}f'^2\right). \tag{16}$$

The boundary conditions to be satisfied are

$$\begin{cases} f(x,\eta)=f'(x,\eta)=0,\;\; \theta(x,\eta)=1 & \text{at}\;\; \eta=0,\\ f'(x,\eta)=0,\;\; \theta(x,\eta)=0 & \text{as}\;\; \eta\to\infty. \end{cases} \tag{17}$$

In the above equations a prime denotes differentiation with respect to η, i.e., $f'(x,\eta) = \frac{\partial f(x,\eta)}{\partial \eta}$ and $\theta'(x,\eta) = \frac{\partial \theta(x,\eta)}{\partial \eta}$. The dimensionless surface shear-stress and rate of heat transfer in terms of the local skin-friction Cf_x and the local Nusselt number Nu_x, respectively, are defined as

$$Cf_x=\frac{2\tau_\mathrm{w}}{\rho U_\infty^2},\quad \text{where}\;\; U_\infty=\frac{\mu_\infty \mathrm{Gr}^{\frac{1}{2}}}{\rho L},$$

and

$$\mathrm{Nu}_x=\frac{x\,q_\mathrm{w}}{k\,(T_\mathrm{w}-T_\infty)}.$$

The quantities of physical interest are the surface shear-stress and rate of heat transfer which may be described in terms of the local skin-friction Cf_x and the local Nusselt number Nu_x, respectively, in non-dimensional form from the relations

$$Cf_x=2\left(\frac{1-\sigma_x^2}{1+\varepsilon}\right)\left(\frac{\mathrm{Gr}}{x}\right)^{-\frac{1}{4}}f''(x,0), \tag{18}$$

$$\mathrm{Nu}_x=-x^{\frac{3}{4}}\mathrm{Gr}^{\frac{1}{4}}\left(1+\sigma_x^2\right)^{\frac{1}{2}}\theta'(x,0). \tag{19}$$

Also, it is worth mentioning that the corresponding expressions in [18] (equations (17) and (18)), are different to the present work.

To initiate the process at $x=0$, we prescribe the profiles for the functions f, θ, and their derivatives from the solutions of the equations

$$\left(\frac{1}{1+\varepsilon\theta}\right)f''' + \frac{3}{4}ff'' - \frac{1}{2}f'^2 - \frac{\varepsilon}{(1+\varepsilon\theta)^2}\theta' f'' + \theta = 0, \tag{20}$$

$$\frac{1}{\mathrm{Pr}}\theta'' + \frac{3}{4}f\theta' = 0, \tag{21}$$

satisfying the boundary conditions

$$\begin{cases} f(\eta) = f'(\eta) = 0, \;\; \theta(\eta) = 1 & \text{at} \;\; \eta = 0, \\ f'(\eta) = 0, \;\; \theta(\eta) = 0 & \text{as} \;\; \eta \to \infty. \end{cases} \tag{22}$$

Table 1. Represents comparison of numerical values of skin friction and Nusselt number for Prandtl number (Pr = 10) against viscosity parameter ε with Hossain et al. [18]

ε	$f''(0)$ Hossain et al. [18]	Present work	$-\theta'(0)$ Hossain et al. [18]	Present work
0.0	0.591	0.592678	0.825	0.826642
1.0	0.975	0.976952	0.931	0.931709
2.0	1.288	1.290630	0.997	0.997935

The nonlinear interactions among the governing continuity, momentum, and energy conservation partial differential equations (15)–(16) are transformed into a linear algebraic system and have been solved numerically with the boundary conditions (17) by using an implicit Chebyshev pseudospectral procedure (the spatial derivatives are computed with a differentiation matrix by using Chebyshev collocation method, and the time derivatives are computed with the Crank–Nicolson implicit finite-difference method; see Elgazery [19]). The computer program of the numerical method and the numerical computations have been done by the symbolic computation software Mathematica 5.2$^{\mathrm{TM}}$ running on a PC. Also, the solution of the above equations (20)–(21) with boundary conditions (22) are obtained using the Newton–Raphson iteration technique and these are entered in Table 1 for different values of the governing parameters. The present results are compared to those obtained by Hossain et al. [18]. It was found that the present results agree very well with the previous results.

3. Results and Discussion

In this section, a comprehensive numerical parametric study is conducted and the results are reported in terms of graphs. This is done in order to illustrate special features of the solutions. So the numerical solution, by using the Chebyshev collocation method in η-direction and the Crank–Nicolson method in x-direction, was obtained for distributions of the dimensionless velocity $f'(x,\eta)$ and the dimensionless temperature $\theta(x,\eta)$ as well as the local skin-friction coefficient Cf_x and the local Nusselt number Nu_x. To study the behaviour of these profiles, curves are drawn for various values of the parameters that describe the flow, e.g. the Eckert number Ec, the Prandtl number Pr, the magnetic parameter M, and the amplitude-wavelength ratio α. It has to be noticed that the values of the parameter set, which are representing a realistic case, are taken from [18]. In Figures 11–16, for example, the value $\mathrm{Pr} = 7$ corresponds to water at approximately 20 °C. Under these circumstances the density ρ of water, the specific heat at constant pressure c_{p}, the kinematic viscosity ν_∞, and the volumetric coefficient of the thermal expansion β_{T} are equal to (see Cebeci and Bradshaw [21] p. 467) $\rho = 1000.52\,\mathrm{kg/m^3}$, $c_{\mathrm{p}} = 4.1818\,\mathrm{K\,J\,kg^{-1}\,k^{-1}}$, $\nu_\infty = 1.006 \cdot 10^{-6}\,\mathrm{m^2\,sec^{-1}}$, and $\beta_{\mathrm{T}} = 0.18 \cdot 10^{-3}\,\mathrm{k^{-1}}$ respectively, the wavelength of the wavy surface amounts to $L = 0.237$ m, and according to its definition, the Eckert number $\mathrm{Ec} = \frac{g\beta_{\mathrm{T}}L}{c_{\mathrm{p}}}$ ($g = 9.81\,\mathrm{m\,sec^{-2}}$) takes the value $\mathrm{Ec} = 10^{-7}$. These values of studied parameters are shown in Figures 2–16.

First of all, a comparison between the values of the skin-friction $f''(0)$ and Nusselt number $-\theta'(0)$ computed by Hossain et al. [18] and their corresponding numerical results for the Prandtl number (Pr = 10) against ($\varepsilon = 0, 1, 2$) are given in Table 1. Also, a comparison between the values of $-\theta'(x,0)$ of the curves computed by Hossain et al. [18] (Fig. 4 b) and their corresponding numerical results for $\alpha = 0.3$, $\varepsilon = 3$, $M = 0$, and $\mathrm{Ec} = 0$ is given in Figure 2. As is evident from Table 1 and Figure 2, it can be concluded that there is great agreement between the results of the skin-friction $f''(0)$, Nusselt number $-\theta'(0)$, and the values of $-\theta'(x,0)$ using the two methods of calculations. In addition, the obtained results using the present method indicate that it is an adequate scheme for the solution of the present problem.

The calculated velocity f' and temperature θ corresponding to parameter values of $x = 25$, $\mathrm{Pr} = 7$, $\alpha = 0.2$, $\varepsilon = 1$, and $M = 1$ for different Eckert number Ec ranged from 0 to 10^{-6} are shown in Figures 3 and 4. The velocity values showed two stages. In the first stage, the velocity increased untill $\eta \approx 1$ while in

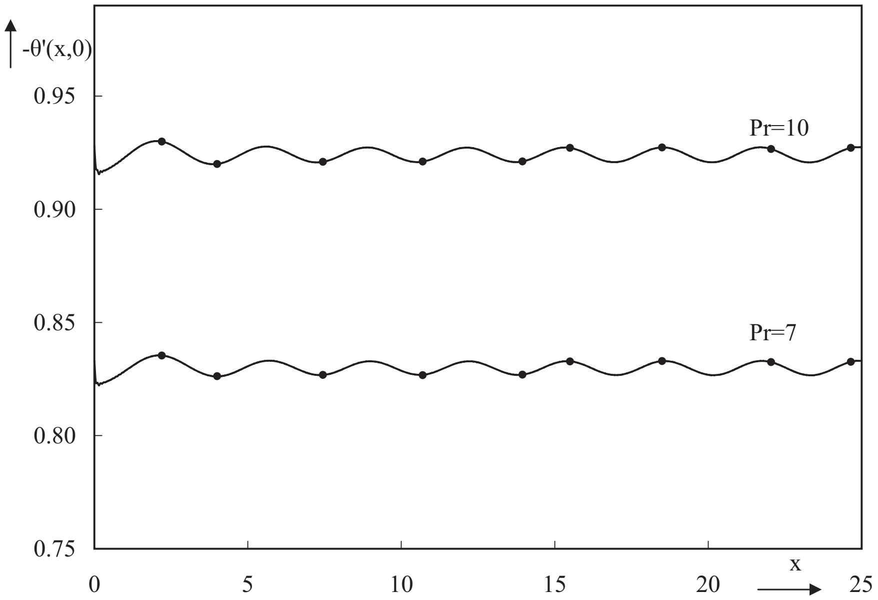

Fig. 2. Comparison of $-\theta'(x,0)$ for different values of Prandtl number Pr with Hossain et al. [18] at $\alpha = 0.3$, $\varepsilon = 3$, $\mathrm{Ec} = 0$, and $M = 0$.

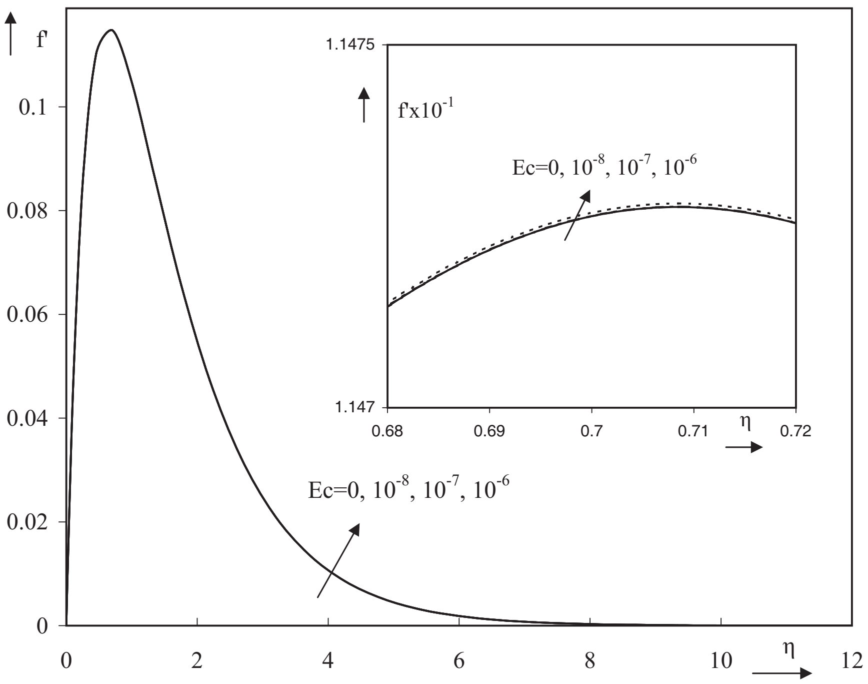

Fig. 3. Effect of Eckert number Ec on velocity distribution at $x = 25$, $\mathrm{Pr} = 7$, $\alpha = 0.2$, $\varepsilon = 1$, and $M = 1$ (the inset shows a zoom of curves).

the second stage, the velocity decreased with further increase of η. The temperature decreased abruptly by increasing the distance η. It reached approximately zero at $\eta = 8$. Also, the calculated $f''(x,0)$ and $-\theta'(x,0)$ corresponding to parameter values of $\mathrm{Pr} = 7$, $\alpha = 0.2$, $\varepsilon = 1$, and $M = 1$ for different Eckert

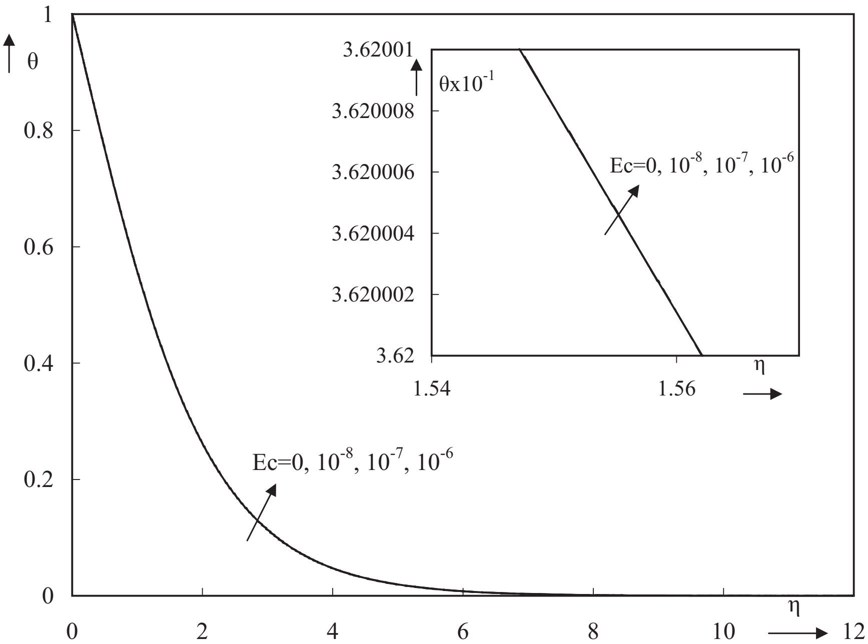

Fig. 4. Effect of Eckert number Ec on temperature distribution at $x = 25$, $\Pr = 7$, $\alpha = 0.2$, $\varepsilon = 1$, and $M = 1$ (the inset shows a zoom of curves).

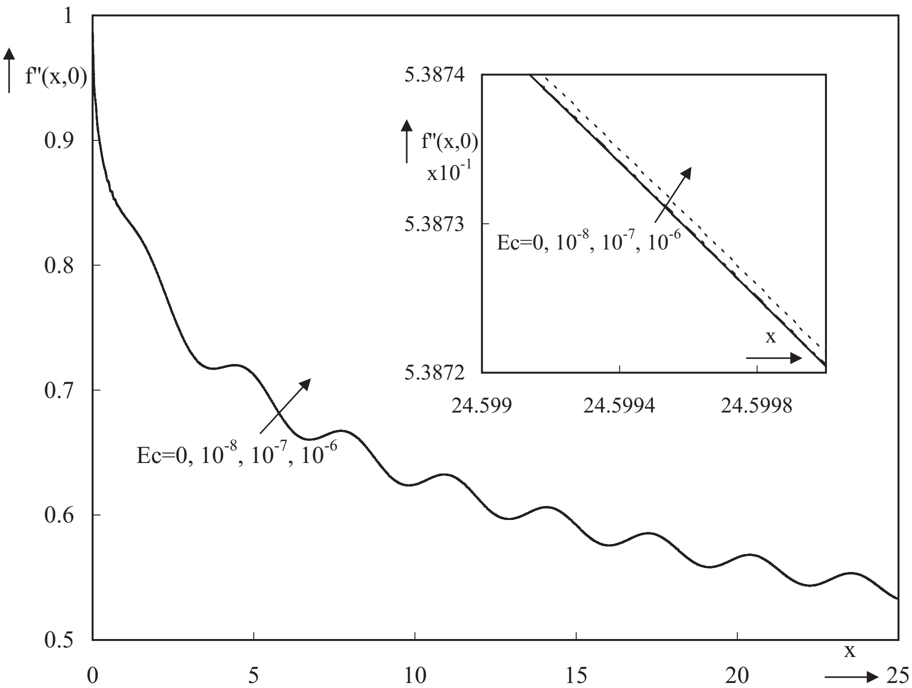

Fig. 5. Effect of Eckert number Ec on $f''(x,0)$ at $\Pr = 7$, $\alpha = 0.2$, $\varepsilon = 1$, and $M = 1$ (the inset shows a zoom of curves).

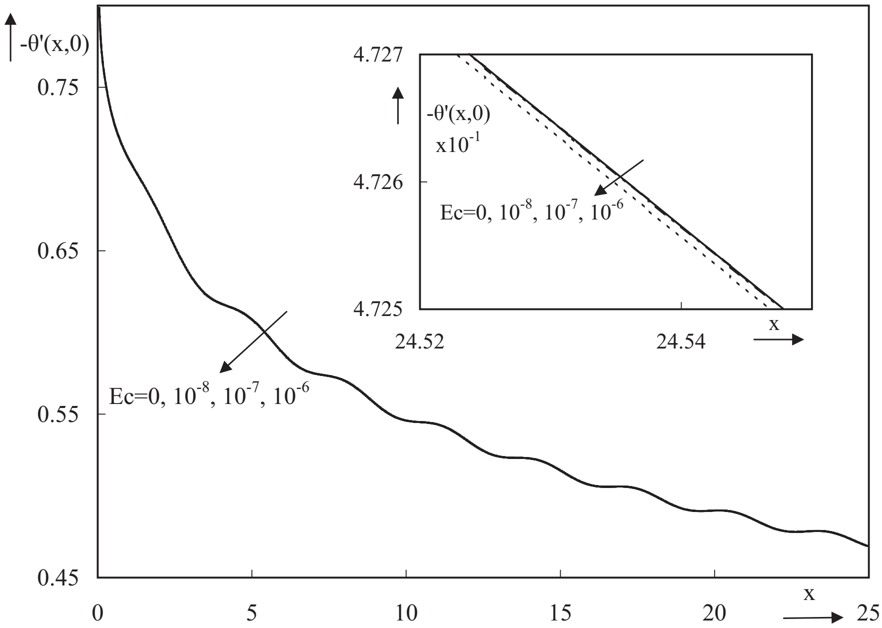

Fig. 6. Effect of Eckert number Ec on $-\theta'(x,0)$ at Pr $= 7$, $\alpha = 0.2$, $\varepsilon = 1$, and $M = 1$ (the inset shows a zoom of curves).

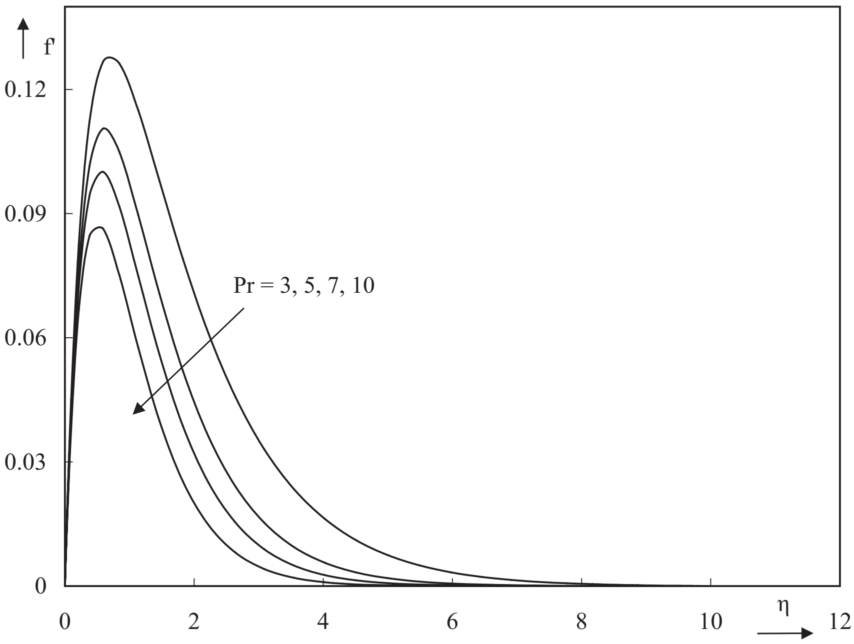

Fig. 7. Effect of Prandtl number Pr on velocity distribution at $x = 25$, Ec $= 10^{-7}$, $\alpha = 0.2$, $\varepsilon = 1$, and $M = 1$.

number Ec ranged from 0 to 10^{-6} are shown in Figures 5 and 6. It is clear that $f''(x,0)$ and $-\theta'(x,0)$ decreased abruptly by increasing the distance x. As shown in Figures 3–6 it is obvious that Ec has minor effects on f', $f''(x,0)$, and $-\theta'(x,0)$. On the other hand, Ec has no effect on the temperature θ. It is clear that with increasing Ec the velocity f' and $f''(x,0)$ distributions increase as shown in Figures 3 and 5 whereas it is observed that $-\theta'(x,0)$ decreases as Ec increases as shown in Figure 6.

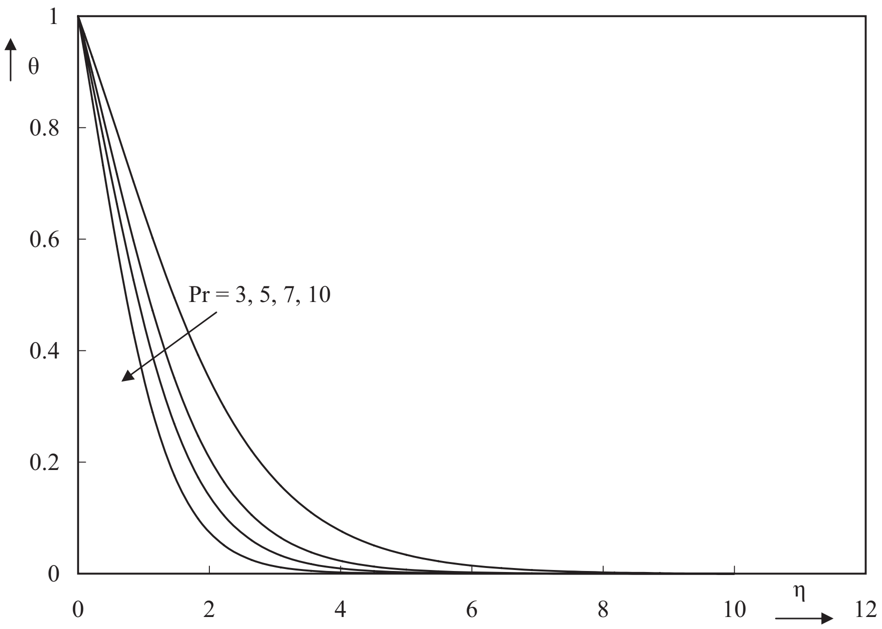

Fig. 8. Effect of Prandtl number Pr on temperature distribution at $x = 25$, $\mathrm{Ec} = 10^{-7}$, $\alpha = 0.2$, $\varepsilon = 1$, and $M = 1$.

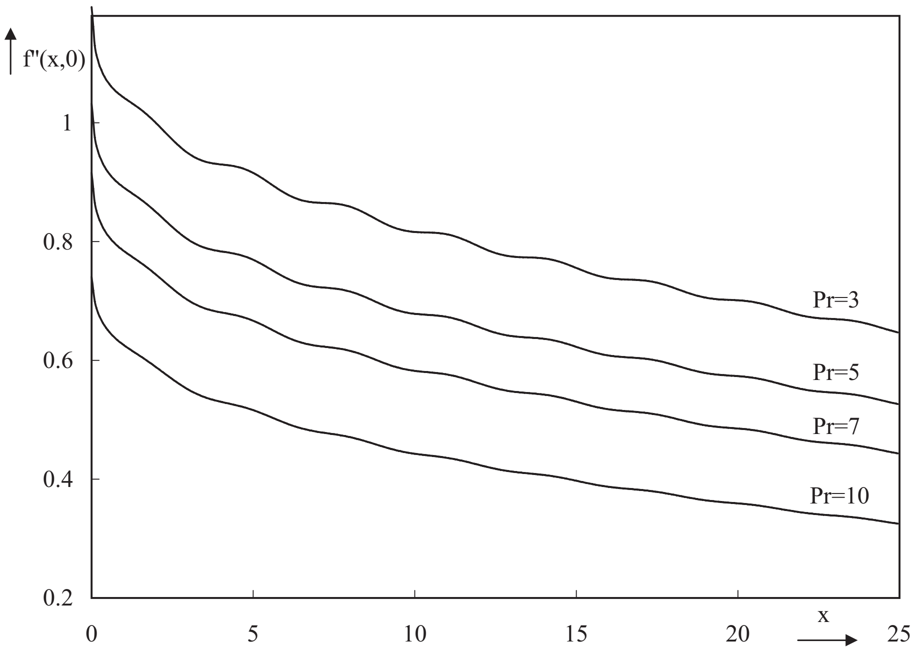

Fig. 9. Effect of Prandtl number Pr on $f''(x,0)$ at $\mathrm{Ec} = 10^{-7}$, $\alpha = 0.2$, $\varepsilon = 1$, and $M = 1$.

Figure 7 shows profiles of the velocity f' as a function of η for different Prandtl numbers Pr arranged from 3 to 10. These velocity profiles were obtained for $\mathrm{Ec} = 10^{-7}$, $\alpha = 0.2$, $\varepsilon = 1$, $x = 25$, and $M = 1$. In general, the distributions of f' were nonlinear for all Prandtl number values. The velocity f' decreased as Pr was increased. Also the maximum values of f' decreased as Pr was increased. Moreover, it is noted that the crest of f' moved downwards as the Prandtl number was increased. Figure 8 displays results for the

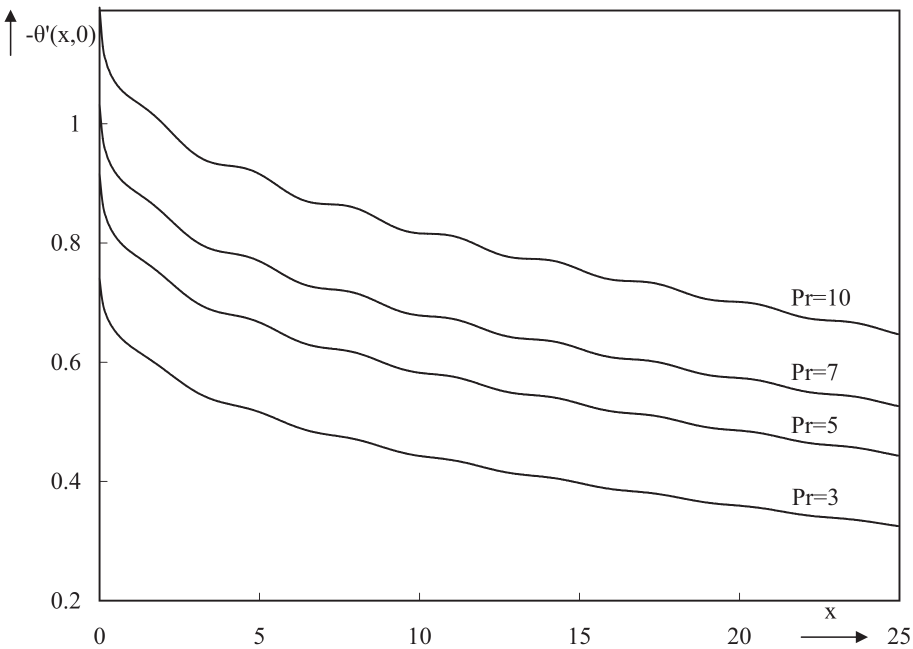

Fig. 10. Effect of Prandtl number Pr on $-\theta'(x,0)$ at $\mathrm{Ec} = 10^{-7}$, $\alpha = 0.2$, $\varepsilon = 1$, and $M = 1$.

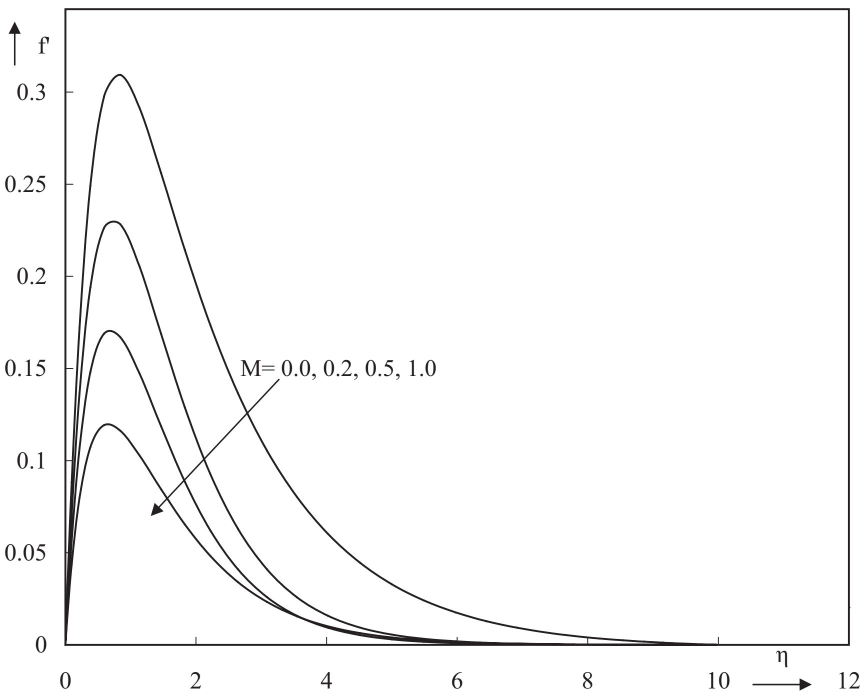

Fig. 11. Effect of magnetic parameter M on velocity distribution at $x = 25$, $\mathrm{Ec} = 10^{-7}$, $\alpha = 0.2$, $\varepsilon = 1$, and $\mathrm{Pr} = 7$.

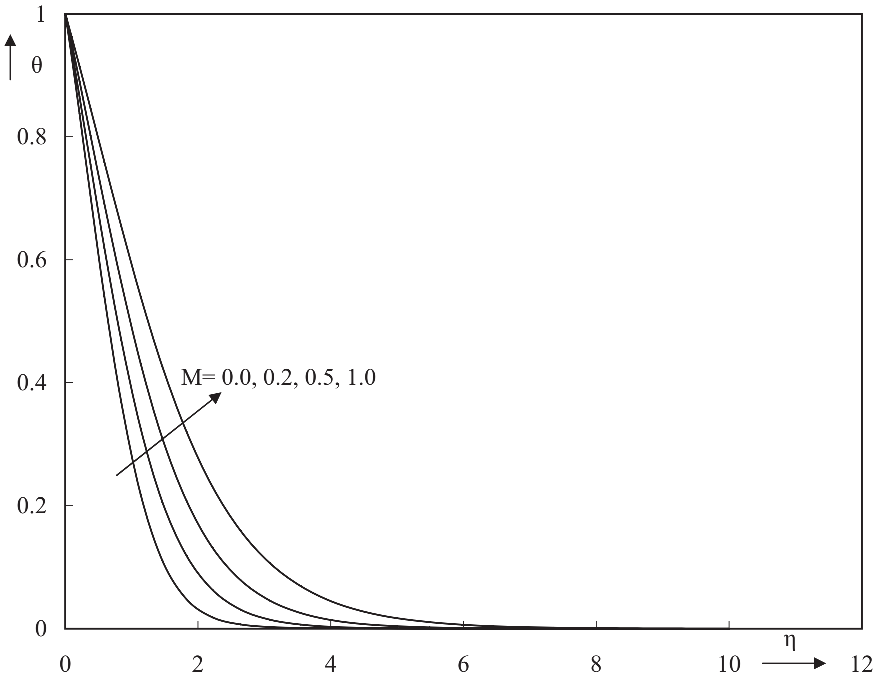

Fig. 12. Effect of magnetic parameter M on temperature distribution at $x = 25$, $\mathrm{Ec} = 10^{-7}$, $\alpha = 0.2$, $\varepsilon = 1$, and $\mathrm{Pr} = 7$.

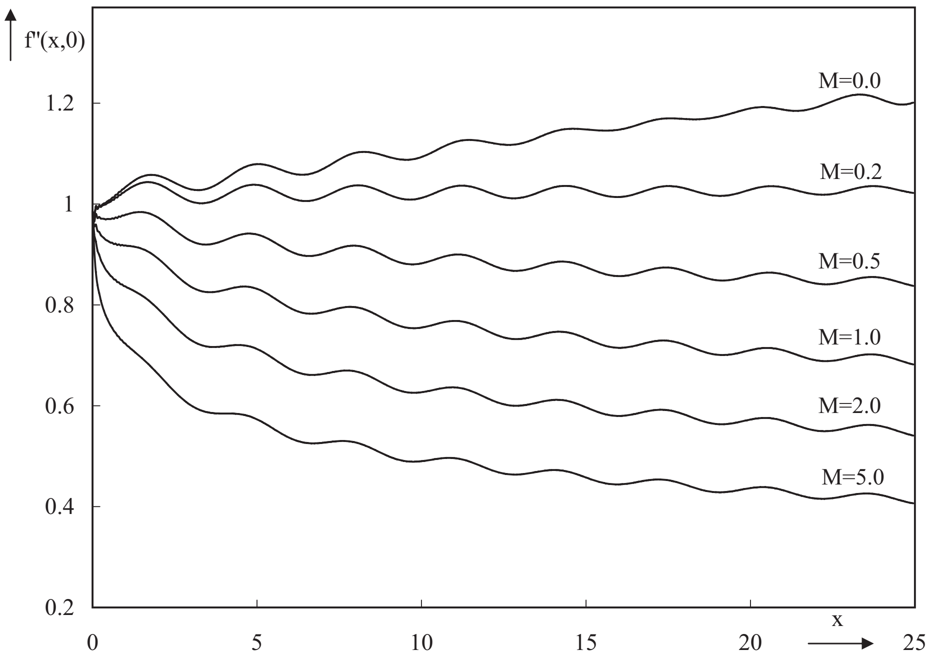

Fig. 13. Effect of magnetic parameter M on $f''(x,0)$ at $\mathrm{Pr} = 7$, $\alpha = 0.2$, $\varepsilon = 1$, and $\mathrm{Ec} = 10^{-7}$.

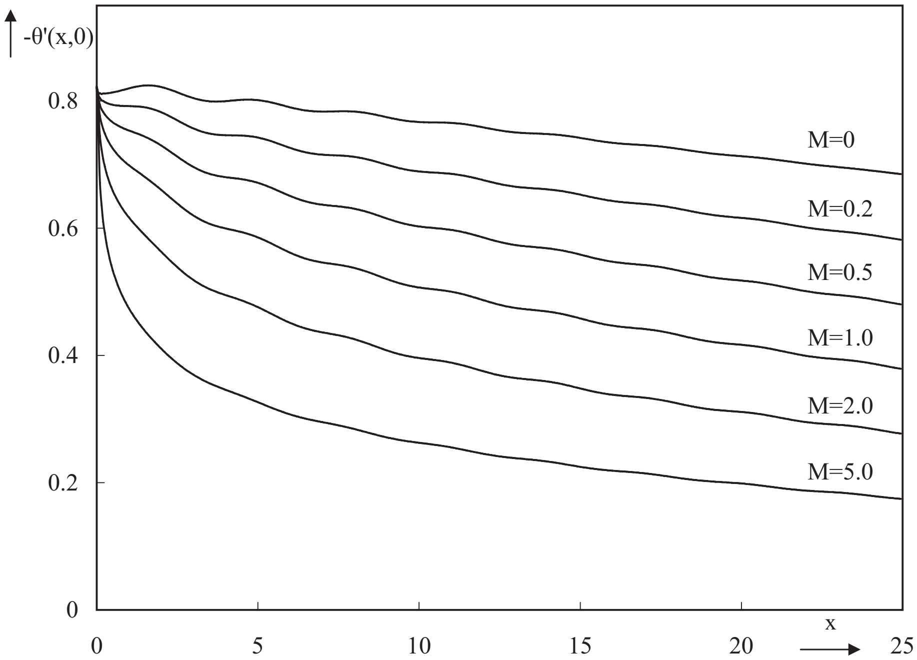

Fig. 14. Effect of magnetic parameter M on $-\theta'(x,0)$ at Pr = 7, $\alpha = 0.2$, $\varepsilon = 1$, and Ec $= 10^{-7}$.

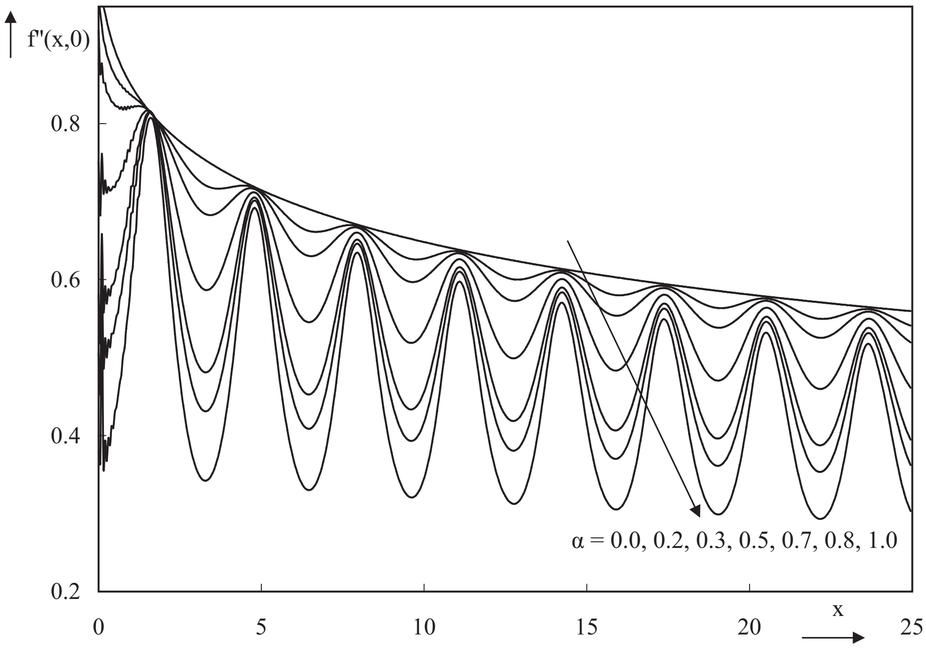

Fig. 15. Effect of surface amplitude parameter α on $f''(x,0)$ at Pr = 7, Ec $= 10^{-7}$, $\varepsilon = 1$, and $M = 1$.

dimensionless temperature θ as a function of η for different Pr arranged from 3 to 10. These temperature profiles were obtained for Ec $= 10^{-7}$, $\alpha = 0.2$, $\varepsilon = 1$, $x = 25$, and $M = 1$. It is clearly seen that as Pr increases the temperature profiles decreases. This is in agreement with the physical fact that the thermal

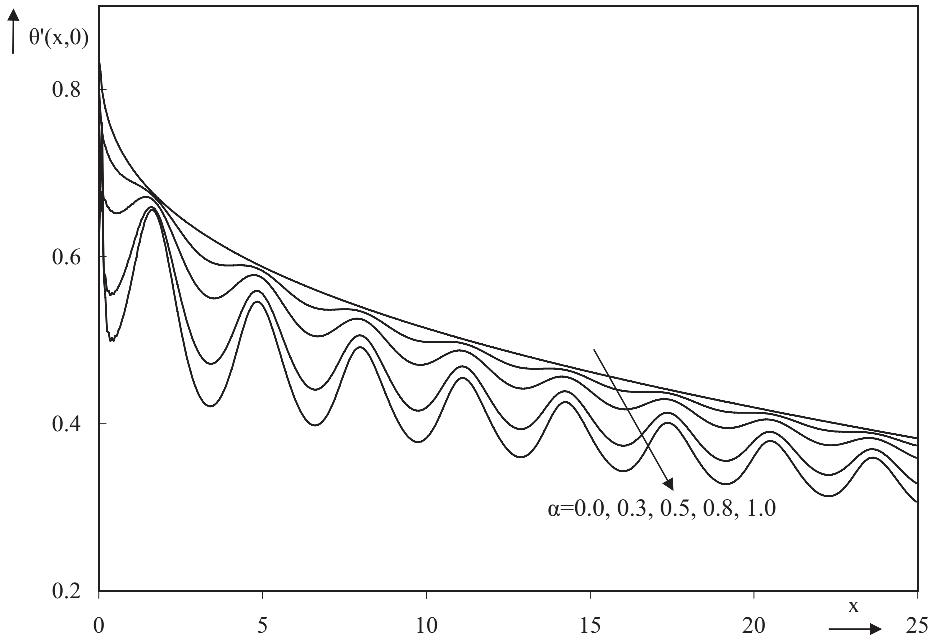

Fig. 16. Effect of surface amplitude parameter α on $-\theta'(x,0)$ at $\mathrm{Pr}=7$, $\mathrm{Ec}=10^{-7}$, $\varepsilon=1$, and $M=1$.

boundary layer thickness decreases with increasing Pr. In other words, the increase in the value of Pr speeds up the decay of the temperature field away from the heated surface with a consequent increase in the rate of heat transfer and a reduction in the thermal boundary layer thickness. Figures 9 and 10 show profiles of $f''(x,0)$ and $-\theta'(x,0)$ as a function of$x$ for $\mathrm{Ec}=10^{-7}$, $\alpha=0.2$, $\varepsilon=1$, and $M=1$ in the region $0\le x\le 25$ for different Pr arranged from 3 to 10. In Figure 9 it has been found that $f''(x,0)$ decreases with increasing Prandtl number Pr whereas in Figure 10 it has been noticed that $-\theta'(x,0)$ increases with increasing Prandtl number Pr.

Figures 11–14 illustrate the influence of the magnetic parameter M on the velocity f', the temperature θ, $f''(x,0)$ and $-\theta'(x,0)$ distributions. It is observed that with increasing magnetic parameter M the velocity distribution decreases as shown in Figure 11 whereas the temperature distribution increases as shown in Figure 12. Also, from Figure 13 it is observed that as the magnetic parameter M increases the $f''(x,0)$ distribution decreases. Moreover, it has been noticed that the $-\theta'(x,0)$ distribution decreases with increasing magnetic parameter M as shown in Figure 14. On the other hand, the application of a transverse magnetic field to an electrically conducting fluid gives rise to a resistive-type force called the Lorentz force. This force has the tendency to slow down the motion of the fluid in the boundary layer and to increase its temperature (as shown in Fig. 12). Also, it is observed that the Ohmic heating (Joule heating) effect due to the effects on electromagnetic work is found to produce an increase in the fluid temperature and thus a decrease in the surface temperature gradient (as shown in Fig. 14). Further, it is found that the effect of viscous heating leads to an increase in the temperature; this effect is more pronounced in the presence of the magnetic field.

Finally, Figures 15 and 16 show how variations in the amplitude-wavelength ratio parameter α affect $f''(x,0)$ and $-\theta'(x,0)$ profiles when $\mathrm{Pr}=7$, $\mathrm{Ec}=10^{-7}$, $\varepsilon=1$, and $M=1$. It is clear that with increasing amplitude-wavelength ratio parameter α both of the $f''(x,0)$ and $-\theta'(x,0)$ distributions decrease.

4. Conclusions

An implicit Chebyshev collocation method has been used to compute the effects of viscous dissipation and Ohmic heating (Joule heating) on MHD natural-convection flow of a temperature dependent viscosity from a vertical wavy surface. By using the present numerical method, a simple coordinate transformation to transform the complex wavy surface into a flat plate was implemented. Boundary layer and Boussinesq approximations have been introduced together to describe the flow field. The system of nonlinear partial differential equations have been transformed into a nonlinear algebraic system by using the Chebyshev collocation method in η-direction and the Crank–Nicolson method in x-direction. The effects of different physical values of the dimensionless parameters that describe the flow like the Eckert number, Prandtl number, MHD variation, and the amplitude-wavelength ratio on the flow have been discussed. It has been concluded from the previous results:

i) With increasing Eckert number the velocity and the $f''(x,0)$ distribution increase, while the $-\theta'(x,0)$ distribution decreases.

ii) With increasing the strength of the applied magnetic field decelerates the fluid motion along the wavy wall inside the boundary layer.

iii) The applied magnetic field tends to impede the motion of the fluid and make it warmer. Thus it reduce the surface friction force.

iv) Increasing the amplitude-wavelength ratio parameter resulted in decreasing the $f''(x,0)$ and $-\theta'(x,0)$ distributions.

v) The results of the velocities showed the changes in its shape from a position close to the boundary layer to a position close to the free stream.

[1] Lun-Shin Yao, ASME J. Heat Transfer **105**, 465 (1983).

[2] S. G. Moulic and L. S. Yao, ASME J. Heat Transfer **111**, 1106 (1989).

[3] D. A. S. Rees and I. Pop, ASME J. Heat Transfer **116**, 505 (1994).

[4] I. Pop and T. Y. Na, Int. Commun. Mass Transfer **21**, 891 (1994).

[5] J. H. Jang, W. M. Yan, and H. C. Liu, Int. J. Heat Mass Transfer **46**, 1075 (2003).

[6] J. H. Jang and W. M. Yan, Int. J. Heat Mass Transfer **47**, 419 (2004).

[7] J. H. Jang and W. M. Yan, Int. J. Heat Mass Transfer **47**, 3695 (2004).

[8] B. V. Rathish Kumar and Shalini, Int. J. Eng. Sci. **41**, 1827 (2003).

[9] B. V. Rathish Kumar and Shalini, Int. J. Heat Mass Transfer **47**, 2353 (2004).

[10] Lun-Shin Yao, Int. J. Heat Mass Transfer **49**, 281 (2006).

[11] M. A. Hossain and I. Pop, Arch. Mech. **48**, 813 (1996).

[12] M. A. Hossain, K. C. A. Alam, and D. A. S. Rees, Appl. Mech. Eng. **1**, 555 (1997).

[13] M. M. Molla, M. A. Hossain, and L. S. Yao, Int. J. Thermal Sci. **43**, 157 (2004).

[14] M. A. Hossain and D. A. S. Rees, Acta Mechanica **136**, 133 (1999).

[15] N. G. Kafoussias and E. W. Williams, Acta Mechanica **110**, 123 (1995).

[16] N. G. Kafoussias, D. A. S. Rees, and J. E. Daskalakis, Acta Mechanica **127**, 39 (1998).

[17] M. A. Hossain, M. S. Munir, and I. Pop, Int. J. Therm. Sci. **40**, 366 (2001).

[18] M. A. Hossain, S. Kabir, and D. A. S. Rees, Z. Angew. Math. Phys. **53**, 48 (2002).

[19] N. S. Elgazery, Commun. Nonlinear. Sci. Numer. Simul. **13**, 728 (2008).

[20] J. X. Ling and A. Dybbs, Forced convection over a flat plate submersed in a porous medium: variable viscosity case. Paper 87-WA/HT-23, ASME, New York 1987.

[21] T. Cebeci and P. Bradshaw, Physical and Computational Aspects of Convective Heat Transfer, Springer-Verlag, New York 1984.